Journal of Technology and System Information Vol: 2, No 4, 2025, Page: 1-17

Multi-classification for Predicting Alzheimer's Disease Using 1.5T1-weighted MRI Imaging and Deep Learning 2D CNN

Shahad Haitham Ali

Middle Technical University

DOI:
https://doi.org/10.47134/jtsi.v2i4.4987
*Correspondence: Shahad Haitham Ali
Email: shahad.haitham@mtu.edu.iq

Received: 30-07-2025
Accepted: 30-08-2025
Published: 30-09-2025

Abstract: Medical imaging holds the pivotal role in clinical diagnosis, education, research work, and treatment of medicine. Medical professionals are tasked with analyzing and interpreting high-level medical data, which is extremely difficult in nature due to the intricate nature of medical images. Deep learning techniques are emerging as strong tools, yielding promising and correct results in the analysis of medical data. Alzheimer's disease, which affects one in every ten individuals aged 65 and above, is a central focus where such advancements are aimed. Artificial intelligence has proved capable of distinguishing between healthy brains and Alzheimer's disease-affected brains. The etiology of the disease lies in abnormal proteins accumulating inside and outside neuronal cells, causing irreparable loss of memory. Alzheimer's disease is the most prevalent form of dementia, and "Mild Cognitive Impairment" (MCI) typically presents as an early indicator, identifying patients who are at higher risk of Alzheimer's disease. However, not all MCI patients go on to develop Alzheimer's, and this highlights the importance of effective interventions. While some patients with MCI (MCI-nc) remain stable, others will progress to Alzheimer's disease. Here, a CNN model was designed and trained first with four classifiers and later retrained with five classifiers. The accuracy rate of the four-classifier model was 98%, while that of the five-classifier model was slightly higher with an accuracy of 98.67%.

Keywords: Magnetic Resonance Imaging, Multi-classification, 2D-CNN, Image Enhancement Algorithms, Alzheimer's Disease. Algorithm Deep Learning, AD, MCI, Predicting.

Introduction

Alzheimer's disease (AD) is the most prevalent form of dementia and accounts for 60–80% of dementia. Protein accumulation within and near neurons is the usual first indicator of the disease, leading to a permanent reduction in memory ability. It is marked by synaptic loss, shrinkage of the brain, and neuronal death. The disease typically becomes noticeable in middle or late life. Even before cognitive impairment starts, the brain also undergoes structural change, and during this first stage, some of the very crucial biomarkers may become abnormal. Research shows that alterations

associated with AD can start 20 years or even more before the onset of clinical symptoms. During early AD, patients have MCI. MCI is a phase of memory loss between typical age-related cognitive decline and the onset of AD (Yang et al, 2017). The estimated 20 to 50% of individuals over the age of 65 years with restrained intellectual impairment have 30 to 40% of them develop AD within five years. Although MCI to Alzheimer's usually develops a mean of 18 months, it may develop in the range of 6 to 36 months. MCI patients either become cases of Alzheimer's disease (MCI-c) or remain stable (MCI-NC), depending on whether the patient has or not developed AD in the earlier 18 months (Ebrahimighahnavieh et al, 2020). MCI is reported to be a prodrome of AD. The pathophysiologic progression of AD may begin years or even decades before scientific analysis. It begins asymptomatic and evolves to the stage of MCI. Early detection, preclusion, monitoring, and prognosis of AD are therefore mandatory. Early intervention may prevent or retard the advancement of neurodegeneration (Zhang et al, 2020).

Alzheimer's disease patients exhibit a significant decline in intellectual function, which has negative implications for their health and well-being. Unlike other neurological disorders, AD treatment has been said to bear a heavy economic burden in nations such as Asia, North America, and globally. The world cost of living with dementia is expected to hit 2.0 trillion USD (Feng et al, 2020) by the year 2030. One of the most significant points of emergence in the pathogenesis of Alzheimer's disease is mild cognitive impairment (MCI), currently increasingly recognized as an onset stage of AD. MCI is a potential candidate for early intervention therapy to potentially reverse, halt, or delay the course of the disease (Amezquita-Sanchez et al, 2019). Studies indicate that approximately 8–15% of MCI patients will progress to Alzheimer's disease each year, whereas 1–2% of individuals who were previously considered to be cognitively healthy will develop Alzheimer's within the same period (Amezquita-Sanchez, 2016). Consequently, early diagnosis is a critical determinant of maximizing clinical outcomes. Surprisingly, current evidence indicates that the likelihood of patients recovering from MCI back to normal cognitive functioning varies according to the duration of follow-up. In clinic-based data, the reversions rate has ranged from 4 to 15%, whereas in population-based data, it has ranged from 29 to 55% (Koepsell & Monsell, 2012), again testifying to the need for early intervention.

Indeed, predictive detection of the onset of AD at an early stage and halting its advancement is vital for future care. Appropriate treatment of AD is dependent on early and accurate diagnosis. If identified at an early stage, patients are able to remain independent for a longer time. One of the primary diagnostic imaging tests is 1.5T1-weighted magnetic resonance imaging (MRI), which is frequently employed to differentiate between individuals suffering from stable MCI-nc and those with MCI-c who are more likely to develop AD. MRI has also been determined to be the primary neuroimaging technique to diagnose Alzheimer's disease and monitor MCI.

In his seminal article on AD at the turn of the 20th century, Alois Alzheimer documented amyloid plaques and neurofibrillary tangles, the histopathological

hallmark of the disease (Alzheimer, 1907). Large modifications in brain histopathology and behavior are hallmarks of AD.

Two main pathological structures which can be seen under a microscope in the AD brain are extracellular amyloid plaques and intraneuronal neurofibrillary tangles. They consist of very insoluble, thick filaments. Amyloid plaques consist of amyloid-β (Aβ) peptides and neurofibrillary tangles by tau protein. Amyloid-β peptides are the proteolytic product of the amyloid precursor protein, while tau is a microtubule-associated protein that is predominantly in axons. AD behavioral symptoms are directly linked to plaque and tangle buildup, destroying and damaging synapses critical for memory and cognition. Synapse loss may result from the inability of living neurons to maintain practical axons and dendrites or due to neuronal death (Bloom et al, 2014).

Related Works

Early diagnosis and accurate classification of AD are important in a bid to embark on effective intervention and treatment. During the recent years, the application of deep learning and sophisticated neuroimaging techniques has had the potential in the domain to enhance diagnostic accuracy. With the utilization of extensive databases like MRI scans, scientists have implemented various models of deep learning in a bid to classify different stages of Alzheimer's disease, including mild cognitive impairment (MCI), which tends to precede AD. This anthology submission recapitulates current studies utilizing deep neural networks and convolutional neural networks (CNNs) in forecasting and diagnosing the onset of Alzheimer's disease using state-of-the-art MRI technique.

In 2018, Medhani Menikdiwela et al. applied deep neural networks for AD classification of two-dimensional cortical surface scans. Considering the reality that AD impacts cortical geometry and thickness, they developed a novel data processing approach that provided comprehensive information on the cortical surface for the purpose of improving early detection. The three-dimensional brain MRI was unfolded to a two-dimensional cortical surface, thickness, curvature, and surface area distributions being combined into an RGB image for insertion into deep networks. Unfolded cortical images within the ADNI dataset were passed through networks like ResNet and Inception. Inception network achieved 81% accuracy in the diagnosis of stable mild cognitive impairment (MCI-nc) and remitting mild cognitive impairment (MCI-c) that is above the 68% accuracy obtained from brain slice images. Such findings highlight the potential of flattened cortical images to enhance Alzheimer's disease diagnosis (Menikdiwela et al, 2018).

Mahjabeen Tamanna Abed et al. employed high-dimensional deep neural network (DNN) models based on transfer learning methodology in 2019 to achieve remarkable results within a short period of time. They employed three different DNN models, VGG19, Inception v3, and ResNet50. Various preprocessing operations were applied to the images, followed by the division of the dataset into training, testing, and validation sets. These DNN models were seeded with weights from pre-trained

models of the ImageNet database. The models were subsequently tested and trained. Following a brief training period of fifteen epochs, the respective accuracy levels were: ResNet50 achieved 70%, Inception v3 achieved 85%, and VGG19 achieved 90%. The data was then used to train various types of Convolutional Neural Networks (CNNs), AD vs. CN classification specifically, and AD vs. MCI vs. CN classification. The images were resized to 224 by 224 pixels, which is a common size to use when training CNNs for the ImageNet dataset. The ImageNet weights were also used, hoping for fast convergence (Abed et al, 2019).

Ali Nawaz et al. (2020) introduced a precise technique for the analysis of AD using a 2D deep convolutional neural network (2D-DCNN) with an imbalanced 3D MRI dataset. They demonstrated that their algorithm, when useful to the AD Neuroimaging Initiative (ADNI) dataset, exhibited improved accuracy, efficiency, and robustness. Data preprocessing included spatial MRI image normalization, intensity normalization, noise removal, correction of bias, contrast, and rescaling using MANGO software. The 3D MRI volumes were also converted into 300 × 300 pixel 2D slices, comprising 67,413 images (20,972 AD, 26,192 MCI, 18,513 NC). The model, with 70 iterations and batch size of 100, used 60% of data for training, 20% for testing, and 20% for validation. Keras framework was employed, with the network architecture including zero-padded convolutional layers, ReLU activation, and five fully connected layers. The model achieved a 99.89% accuracy in predicting AD into three classes.

The Department et al. constructed a deep learning model in 2021 to predict three-year adaptation of mild cognitive impairment (MCI) to AD from longitudinal whole-brain 3D MRI scans. There were 320 samples of 554 controls of normal cognition (NC) and 237 patients of MCI, 3D T1-weighted MRIs at the first diagnosis of MCI and 12-month follow-up. The unsegmented data for cortical thickness or regional structural volumes were split into 75% training and 25% testing. The two methods of transfer learning—zero-shot and fine-tuning—were tried, and the zero-shot method was more successful. CNN models trained with longitudinal data better than single-time MRIs. The best CNN model contained a balanced accuracy of 0.793 in MCI to AD conversion (Ocasio & Duong, 2021).

Swapandeep Kaur et al. employed a deep convolutional neural network (CNN) model in 2022 to classify four stages of Alzheimer's disease (AD): very mild demented, mild demented, average demented, and non-demented. It utilized a training dataset of 5,000 images and an MRI test set of images on Kaggle. The model, which consisted of 40 layers made up of convolutional layers, pooling layers, batch normalization, dropout, flattening, and a fully connected layer, also achieved a classification accuracy of 98.9% in the moderately demented group with a classification error rate of 0.01 and a specificity of 0.992. The model also had the best false positive rate of 0.007 (Kaur et al, 2022).

In 2023, Deevyankar Agarwal et al. used the EfficientNet-b0 convolutional neural network (CNN) with a new fusion technique that merged end-to-end and transfer learning for the diagnosis of several stages of Alzheimer's disease. 245 T1-

weighted MRI scans in cognitively normal (CN), AD, and stable mild cognitive impairment (sMCI) patients were investigated in the study. Preprocessing was carried out using ANtsPyNet packages, including N4 bias field correction, spatially adaptive filtering for denoising, brain extraction from a pre-trained U-Net model, and registration of MRI scans to the MNI152 brain template. Classification reported an accuracy of 95.29% for sMCI vs. AD and 87.38% for multiclass classification of AD vs. CN vs. sMCI (Agarwal et al, 2023).

Methodology

Deep learning (sometimes called deep formal education, deep machine learning, or hierarchy learning) is the learning of neural nets and related learning procedures that involve considerably more than a hidden layer. Learning representations is a subfield in machine learning. Examine numerous levels of representation that correspond to different abstraction levels. Levels can be used to construct a hierarchy of concepts. In a basic scenario, two sets of neurons are present; one group receives an input signal, while the other group sends out a signal.

Every time the input layer receives an input, it also alters it before sending it on to the subsequent layer. Numerous deep learning architectures, such as recurrent neural networks, deep convolution networks, deep belief networks, and deep learning models, have been applied in fields like bioinformatics, speech processing, natural language processing, machine vision, and voice search because they have established exceptional performance in a range of tasks (Ongsulee, 2017). Convolutional Neural Networks (CNNs) have transfigured the arena of computer vision and beyond by introducing models capable of automatically extracting hierarchical features from raw data. Inspired by the visual perception mechanisms in biological systems, CNNs leverage local connectivity, weight sharing, and multi-level abstraction to process images, audio, and even sensor data efficiently (Li et al, 2021).

Components of The CNN Building

In this section, the neural network bypass algorithm (CNN) receives images directly, which has contributed to the successful outcomes. On the other hand, a low-quality image could make it harder for the algorithm to identify and learn. Each class has a picture, and the images are categorized into classes. Each group contains a different amount of photographs, and the aggregates received the same number of images because the images from each class are retained collectively. It has been suggested that multi-layered CNNs can directly recognize trends from the image's pixel units based on force to distribution (Ongsulee, 2017).

A. The Convolution Layer in CNN

The convolutional layer is the core element of any CNN and is responsible for extracting local features from input data. Unlike fully connected layers that connect every neuron to every input, convolutional layers use a set of learnable filters (also

known as kernels) to scan different regions of the input, producing feature maps that represent the activation of each filter at various spatial locations (Li et al, 2021).

Properties of this layer depend upon the number of maps, map sizes, and core sizes. There are M maps of the same size (M, M, C) in each layer representative the networks, width, and height. Additionally, each map in a layer relates to every other map in the layer. The neurones in one map have the same weight values even though their input fields differ. Sharing weights or sharing the kernel with all parts of an image was the most applicable characteristic of the outer approach.

B. Padding Layer

Generally speaking, applying small grains may outcome in the loss of certain pixel elements for some twists, but it may also allow for the use of various convolution layers later on. Adding more pixel elements from padding around the input image borderline is a crucial way to solve this issue and increase the images' effective size (Sarvamangala & Kulkarni, 20220.

C. Pooling type Max-Pooling

The assembly operative has a fixed-form opening, which scans over each input region on its step and produces a single productivity for apiece site that has been covered by the immovable-form window (also called the assembly window). This is the opposite of layer convolution. But there are no filter parameters in the assembly layer, as opposed to computing the lattice layer of association with reverence to the basis and input. Aggregation factors, on the other hand, have been viewed as unavoidable and are calculated as a matter of course as the mean highest value of the parts in the assembly window and named as the mean highest assembly or assembly (Jain et al, 2019).

D. The Regularization of Dropouts

To effectively address the issue of overfitting in neural networks, the process of randomly losing neurons (either visible or hidden) within a neural network is known as "dropout." The withdrawal rate is just the probability of a neuron in a particular layer being dropped. Seepage within the neural network, as restrained by the leak rate of 0, is accountable for the result of any percentage of neurons in a hidden layer. When set at 0, all neurons in a buried layer will reach 0. The anterior transit and back propagation procedures do not incorporate the faulted neurons (Jain et al, 2019).

E. Fully Connection

After several convolution and pooling layers have distilled the spatial features of the input data, fully connected layers (FC layers) serve as the high-level reasoning component of the network. They provide a final mapping from the extracted features to the output predictions (Li et al, 2021). In order for a classifier like Softmax to predict the final labels, the fully connected layers combine the spatial information into a one-dimensional vector. Additionally, the number of output contracts in the last

completely connected layer is comparable to the number of categories (Sarvamangala & Kulkarni, 2022).

F. Non-Linear Layers

Need the instigation function to complete the series of equations because it is the most crucial component of the algorithm for determining the optimal solution. Different kinds of activation functions exist, and each is appropriate for a particular kind of task. A dissimilar type of instigation function was utilized in this study. Each one produced a distinct result, with the superlative instigation function coming out on top (SOFTMAX and ReLU) (Sarvamangala & Kulkarni, 2022).

G. Loss Functions

The above section has explained the varying layers of the CNN architecture. Further, the final classification is derived from the output layer, which is the last layer in the CNN model. Various loss functions are applied in the output layer to compute the error generated through the CNN's training process. This error is the difference between the predicted and actual outputs. The objective of the learning process in the CNN is to minimize this error as much as possible. The loss function relies on two main parameters to determine the error: the predicted output (referred to as the "prediction") and the actual output (referred to as the "label") (Alzubaidi et al, 2021).

Softmax Loss or Cross-Entropy Function: The softmax loss function, alternatively referred to as the cross-entropy function, is extensively used for evaluating the performance of CNN models. It is also called the log loss function. The output of this function is a measure of probability,

p∈{0,1}. The function is most commonly utilized as a substitute for the squared error loss function in multi-class classification. Softmax activation is utilized in the output layer to produce the output in the form of a probability distribution. The mathematical expression for the cross-entropy loss function is given by Eq (Alzubaidi et al, 2021).

$$H(p,y) = -\sum_{i} y_i \log(p_i) \quad where \quad i \in [1,N] \tag{1}$$

1) backpropagation

Using the chain rule for the forward pass, backpropagation is a simple technique that allows the computation of gradients of the loss with respect to the weights. The loss function computes the difference between the network's prediction and the ground truth target value after the network has computed the predictions for a single input example. Backpropagation provides us with a good idea of how the overall loss fares for an infinitesimal change in the weight by computing the loss gradient over weights and biases.

The weights would then need to be updated step by step (in the direction of the negative gradient) in order to reach the local minima. This process of reducing the loss function to achieve the minimum is known as gradient descent. Thus, the network learns (via slow and iterative weight updating) patterns that can minimally and

accurately disagree on any input sample provided. There exist several ways of updating the weights in neural networks via gradient descent (Michelucci, 2018).

2) Deep Learning Optimizers

To reduce a given loss function, optimizers—central deep learning algorithms—adaptive fine-tune a model's parameters during the training process. The techniques allow neural networks to quickly learn and improve by iteratively refining weights and biases based on feedback from data. Core optimizers like Adam, RMSprop, and Stochastic Gradient Descent (SGD) use different update rules, learning rates, and momentum techniques. These adaptive methods are designed to rapidly converge on optimal model parameters to enhance network performance as an entire.

Adaptive Moment (Adam)

Adam optimization algorithm is a proposed optimizer that has been developed for deep learning. It is an amalgamation of RMSProp, momentum, and SGD. Adam uses training data to iteratively update the network weights. Adam uses the regular of the second instants of the inclines to adapt the parameter learning rates, in contrast to RMSProp, which adapts using the typical first instant (the mean) (Michelucci, 2018).

Data Collection

Under the esteemed guidance of Dr. Michael W. Weiner, the Alzheimer's Disease Neuroimaging Initiative (ADNI) was inaugurated in the year 2003 as a collaborative endeavor between public and private sectors. The principal objective of the ADNI initiative is to determine whether sequential magnetic resonance imaging (MRI) scans, in conjunction with positron-emission tomography (PET) imaging, various biological markers, and comprehensive clinical and cognitive assessments, can be employed to monitor the advancement of moderate cognitive impairment (MCI). AD constitutes one specific form of dementia. The comprehensive database may be accessed at the succeeding URL (http://adni.loni.usc.edu/). Brain visualization data from ADNI1, ADNI 2, and ADNI GO was procured for the dataset pertaining to MCI patients subsequent to data access (MRI). The 1.5T1-weight MRI images were preserved in a NIFTI file format, which employs the MP-RAGE protocol to ensure the reliable storage of data.

In instances where MRI images were utilized, three 1.5T1-weighted MRI slices, namely sagittal, axial, and coronal—were employed. The MRI images were classified into several categories: Within a span of six months, MCI-c is anticipated to transition into AD. MCI-nc refers to the classification that did not progress to stable AD, MCI-c, which is expected to convert to AD within 18 months, and MCI-c, which is projected to progress to AD within 12 months, in addition to a category that will ultimately transition into Alzheimer's Disease, albeit the timeframe for this progression has yet to be ascertained. Each classification is represented by its respective category on a scale of (100).

1) Preprocessing of data

Pre-processing is a significant process that focuses on enhancing the quality of images, hence allowing for more effective analysis. It involves removal of unnecessary distortions and enhancement of prominent image features. Pre-processing is included in a series of procedures carried out to prepare images in a proper format prior to being input into the model for optimal performance as well as accuracy.

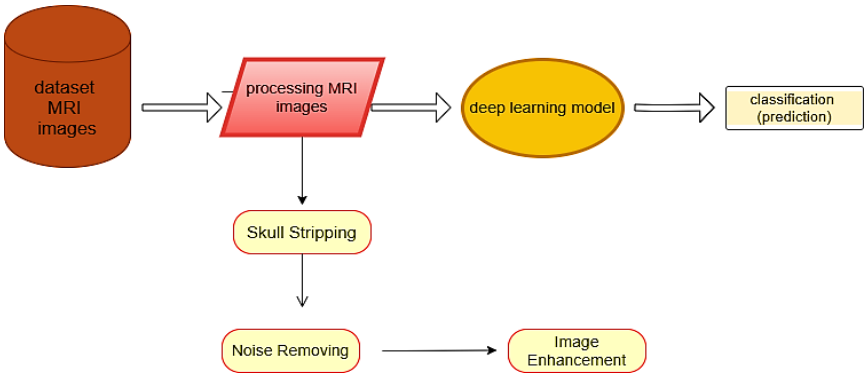

Figure 1. shows data access from the ADNI database, pre-processing steps, and image enhancement after processing

The pre-processing includes the procedures to eliminate the skull in order to excerpt the brain, lower the noise, and enhance the three strips' pictures. The three carpets were first separated from one another following the completion of the

contrasts	alpha	beta
60	1.1	90
70	1	45
80	2	90
90	1	20
100	0.9	10
Greater than 100	1.5	0

procedure The slice sagittal is handled in the manner described below:

Table 1. The slice sagittal

The first phase involves improving the contrast use(Percentage Linear Contrast Stretch) (Muniyappan et al, 2013) (Jensen & Lulla, 1987) in MRI slices—sagittal images and applying (morphological procedures) (Gunturk & Li, 2018). To fill the cavities in the region of interest (object), the closing operation is used. Then, by convolution the structural element as a disk around the region of interest (object), erosion is used to remove non-brain regions, which are represented by the skull. Erosion is then applied once more after the region of interest (object) is isolated from the background using a global threshold. dark parts get bigger while the light portions go smaller due to erosion. The(ots'u threshold procedure) (Yousefi, 2011) is applied to separate the item from the black background to determine the region of interest (the object), and the

associated component labeling technique is used to determine the largest region (Schwenk & Huber, 2015), where each of the three regions is calculated after labeling each object and as a result, the major area will be the mask, and the other regions will be ignored. After that, the shape masking process is applied again, this time to the mask which aims to remove the holes in the selected region. After that, the expansion process is performed on the mask by wrapping the structural element into a disc shape.

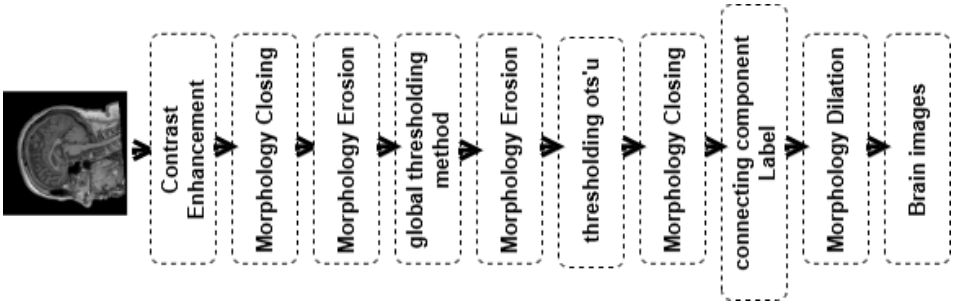

Figure 2. shows the diagram of pre-processing steps (skull stripping) of sagittal slices image from ADNI datasets

Regarding the two slices, the axial and coronal, they underwent distinct preprocessing procedures. In order to differentiate the brain from the skull, the slices' binary brain images were converted from grayscale to binary (black and white) images. The connecting component label was then applied to the binary brain images, giving each section of the brain a distinct color. The region of attention (object) was separated from the circumstantial using the Ots'u procedure, and the largest area was determined while ignoring the other areas in order to represent this with a mask. A closing operation was used to seal the mask's holes and join the cracks in the area of interest. By convolution the structural element in a disk shape around the mask, a dilation operation was applied to improve the mask's shape and make it appropriate for the size of the brain for both slices. The skull was then removed from the brain images by invoking the images of the two slices inside the mask, thus finishing the skull stripping procedure for the three slices.

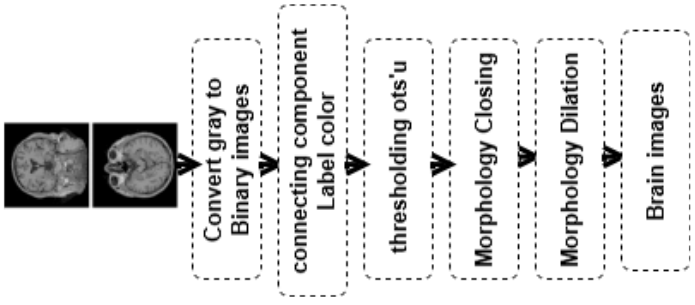

Figure 3. shows the diagram of pre-processing steps (skull stripping) of the axial and coronal slices image from ADNI datasets

2) Noise Removing and Enhance Images

Three different kinds of filters are used in the noise removal techniques the researcher discussed, where the noise makes the classification job more challenging.

Since the data improves after implementation, noise reduction is a crucial step that allows us to see things more clearly.

Prior to eliminating the noise, the ('CLAHE') (Salem et al, 2019) algorithm was employed, designed specifically for enhancing medical images. This algorithm yields improved results compared to standard medical images, as it enhances details in regions that are either darker or lighter than the majority of the image.

$$f(x,y) = \frac{1}{mn} \sum_{(m.n)\in w} I(m.n) \quad (2)$$

Use ('Mean Filter') (Padzil & Crebbin, 2016) In this instance, the filter computes the uncaring of the damaged picture within a specified region. The center value is then used to modify the center pixel density value. Based on a spatial filter, the arithmetic average filter substitutes a sliding window filter for the window's center value Reducing the intensity contrast between two pixels is accomplished with the ('median filter')[31]. In this filter, the median value takes the place of the number of pixels. Next, all of the pixel values are sorted ascending to get the median, and the computed pixels are then replaced with the internal pixel value.

$$f(x,y) = median\{I(m,n)|(m,n) \in W\} \quad (3)$$

('Gaussian Filter') (Owotogbe et al, 2019) Gaussian Blur is the name of the Gaussian filter. The Gaussian filter is a kernel generator according to the Gaussian equation. The kernel is a sophisticated array that is utilized for image-filtering functions like embossing, smoothing, sharpening, and blurring. For Gaussian blur, both filtering and smoothing techniques can be applied (Desai et al, 2020).

$$G(x,y) = \frac{1}{2\pi\sigma^2} e^{-\frac{x^2+y^2}{2\sigma^2}} \quad (4)$$

The brain images underwent preparation for model input by applying a sharpening technique (high-pass filter) following noise reduction. This step is essential for detecting the edges and details of the three brain image slices. This procedure enhances MRI images of the brain, as illustrated in Figure 4.

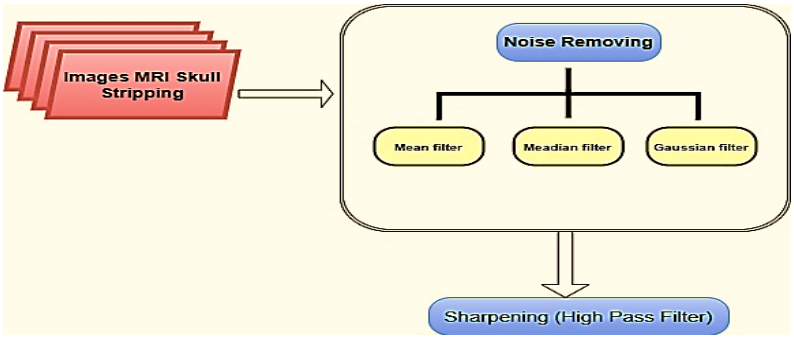

Figure 4. represents the noise removal and image enhancement after the skull stripping of the three slides

CNN Classification (Prediction)

The image was then resized to 64x64 pixels for the purpose of preparing it for input into the model. Various models were made, each with a different number of categories. The first model consisted of four classifiers: (1) MCI-c individuals who will develop AD within six months, (2) MCI-c individuals who will develop AD within twelve months, (3) MCI-c individuals who will develop AD within eighteen months, and (4) individuals who will eventually develop AD but are not expected to convert within the given time intervals. There were five groups in the second model: (1) MCI-c subjects who would develop AD within six months, (2) MCI-c subjects who would develop AD within twelve months, (3) MCI-c subjects who would develop AD within eighteen months, (4) subjects who would develop AD but later, and (5) stable MCI-nc subjects who did not develop AD. The image pixel values were then normalized. As a significant phase in creating neural networks, model configuration consisted of splitting the dataset into two parts, one of which 75% was utilized for preparation and 25% for testing. Convolutional neural networks make use of convolution layers; a single layer is used to spread a convolution kernel over the matrix of the input layer. The input to the CNN is an image with a size of 64x64x3. The image passes through a 2x2 convolutional layer and thereafter gets transformed to a feature map or activation map. The convolutional layers also wrap around the input and feed outputs to subsequent layers. The stride specifies how much the filters move in terms of width and height of the image; that is, a stride one shifts the filters one pixel. The most widely used activation function is ReLU. Convolutional networks may also include aggregation layers, which reduce data dimensionality by pooling the groups of neurons into a single neuron in the subsequent layer. Local pooling uses a 2x2 kernel, and max pooling takes the maximum of each local pool. With several convolutional and aggregation layers, fully connected layers perform the final classification. Fully connected layers connect each neuron in a layer with each neuron in the next layer. The flattened matrix is passed through a fully connected layer. Backpropagation is the primary process of training the neural network, which adjusts the network weights based on the error rate computed at each epoch. By increasing generalization, the optimizer (Adam) lowers the error rate, correctly adjusts the weights, and makes the model dependable, Batch size that was used (32) and (34) of the four-class and the five-class. Dropout was used to disable cells in the hidden layers at 25% and 50% in order to combat overfitting. SOFTMAX classifiers offer the possibilities for each class label for image classification, and its activation function is typically ReLU. Cross-Entropy Loss was used in the two multi-category classifications. The calculation of this function is a convergence comparison of the probability distribution of the scores of the outputs resulting from the model and the expected target group.

Result and Discussion

In order to ascertain four instances of patients exhibiting "mild cognitive impairment" who may potentially advancement to AD, the model was initially subjected to training. These instances encompassed MCI-c patients who could transition to AD after a duration of six months, MCI-c patients who could transition to AD after a duration of twelve months, MCI-c patients who could transition to AD after a duration of eighteen months, and those who could transition to AD but appear to lack sufficient time. Figure 5 elucidates that, when accounting for the number of classified learning attempts (Epoch = 30) and a Batch size of 32, the accuracy achieved was 98%. Utilizing the identical configuration as the initial model, the second model was trained with an additional classification aimed at identifying MCI-nc patients who manifested mild cognitive impairment yet were not at risk of evolving AD. Through learning attempts, the accuracy of the model was recorded at 98.67% (Epoch = 30) with a Batch size of 34. The correlation matrix pertaining to both models is obtainable in Figure 5.

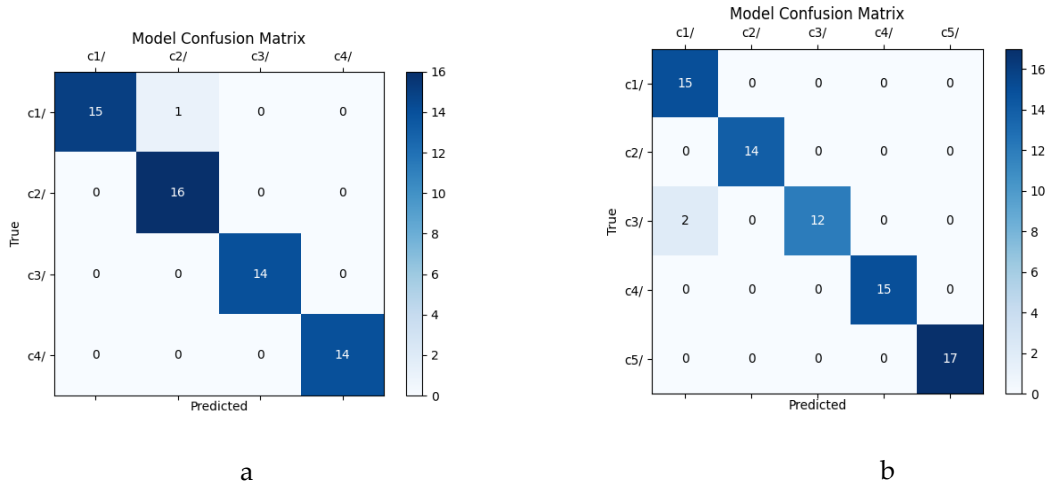

a b

Figure 5. shows the confusion matrix for the 2D-CNN-Softmax model for the(a) 4 and 5(b) classification categories.

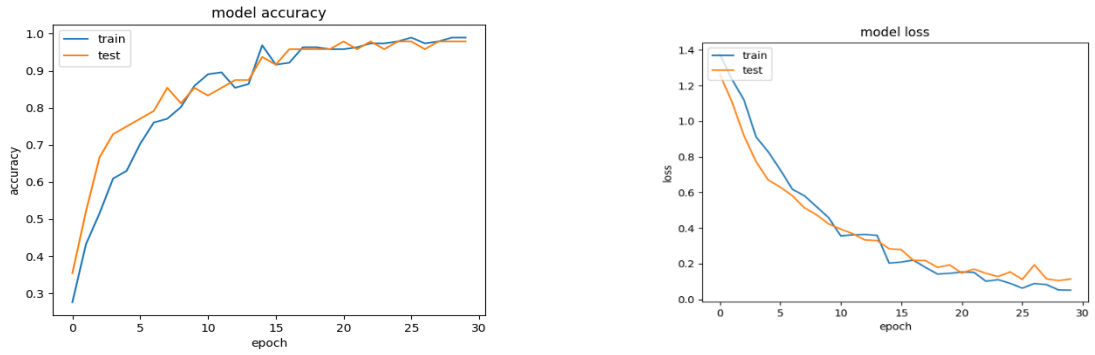

Figure 6. shows the alternative loss model (training and validation accuracy) graph for the 2D-CNN-Softmax model's 4 categorization in (Epoch=30)

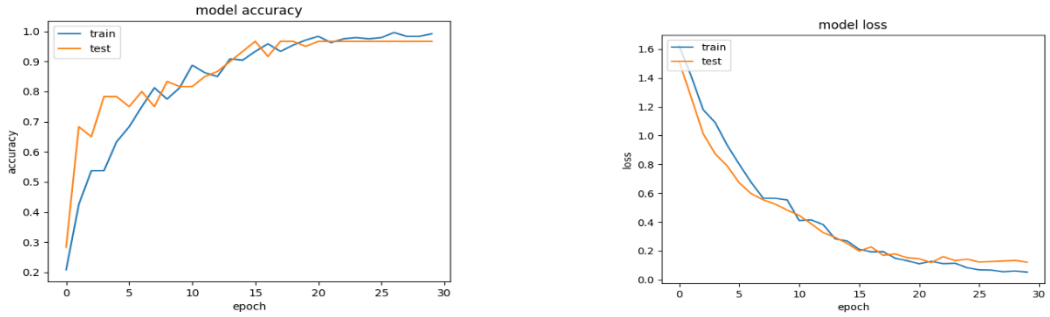

Figure 7. shows the alternative loss model (training and validation accuracy) graph for the 2D-CNN-Softmax model's 5 categorization in (Epoch=30)

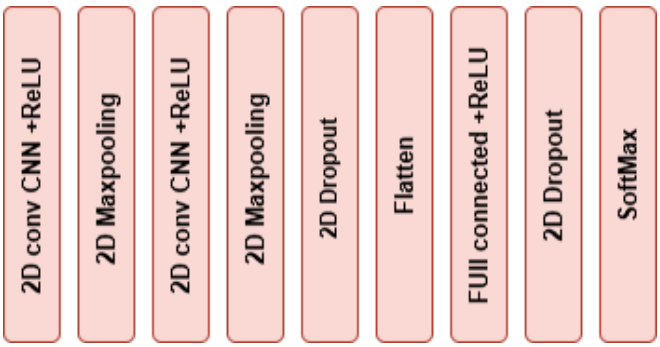

Figure 8. The number of initialized layers for the two models to be trained for classification for 2D-CNN-model

The Outcomes of The Experiment

The arrangement model is built using Kara's, a high-level Python neural network API. the model's overall performance in every category is beneficial when each category is equally significant. Accuracy is calculated as the number of accurate predictions divided by the total number of predictions.

Conclusions

Before neurodegeneration occurs, it is essential to implement preventative strategies and address MCI patients promptly by utilizing 3D MRI images to forecast their progression to Alzheimer's disease. Pre-processing of the images involves skull stripping, and filters such as median and Gaussian are applied to minimize noise in medical images, thus removing the most common noise types. Three-slice MRI images with 1.5T1 weighting are an appropriate format for establishing and executing the 2D-CNN deep learning algorithm model, leading to an efficient classification model. The classification accuracy achieved by the two trained models was 98% for the initial model with four categories and 98.67% for the secondary model with five classifications (Epoch=30).

Acronyms

AD: Alzheimer's disease
Adam: Adaptive Moment Estimation
ADNI: Alzheimer's disease Neuroimaging Initiative
CLAHE: Contrast Limited Adaptive Histogram Equalization
CNN: convolutional Neural Network
MCI: mild cognitive impairment
MCI-c: mild cognitive impairment convert to AD
MCI-nc: mild cognitive impairment NO convert to AD
MRI: Structural Magnetic resonance imaging
NIFTI: Neuroimaging Informatics Technology Initiative
PET: Positron Emission Tomography
ReLU: Rectified Linear Unit

References

Abed, M. T., Nabil, S. A., & Fatema, U. (2019). Early prediction of Alzheimer's disease using convolutional neural network. *Brac University*.

Agarwal, D., Berbís, M. Á., Luna, A., Lipari, V., Ballester, J. B., & de la Torre-Díez, I. (2023). Automated medical diagnosis of Alzheimer's disease using an efficient net convolutional neural network. *Journal of Medical Systems, 47*(1), 57. https://doi.org/10.1007/s10916-023-01913-9

Alzheimer, A. (1907). Ueber eine eigenartige Erkrankung der Hirnrinde. *Allgemeine Zeitschrift für Psychiatrie und Psychisch-Gerichtliche Medizin, 64*, 146–148.

Alzheimer, A., Stelzmann, R. A., Schnitzlein, H. N., & Murtagh, F. R. (1995). An English translation of Alzheimer's 1907 paper: "Über eine eigenartige Erkankung der Hirnrinde." *Clinical Anatomy, 8*(6), 429–431. https://doi.org/10.1002/ca.980080612

Alzubaidi, L., Zhang, J., Humaidi, A. J., Al-Dujaili, A., Duan, Y., Al-Shamma, O., Santamaría, J., Fadhel, M. A., Al-Amidie, M., & Farhan, L. (2021). Review of deep learning: Concepts, CNN architectures, challenges, applications, future directions. *Journal of Big Data, 8*, 53. https://doi.org/10.1186/s40537-021-00444-8

Amezquita-Sanchez, J. P., Adeli, A., & Adeli, H. (2016). A new methodology for automated diagnosis of mild cognitive impairment (MCI) using magnetoencephalography (MEG). *Behavioural Brain Research, 305*, 174–180. https://doi.org/10.1016/j.bbr.2016.03.002

Amezquita-Sanchez, J. P., Mammone, N., Morabito, F. C., Marino, S., & Adeli, H. (2019). A novel methodology for automated differential diagnosis of mild cognitive impairment and Alzheimer's disease using EEG signals. *Journal of Neuroscience Methods, 322*, 88–95. https://doi.org/10.1016/j.jneumeth.2019.05.007

Bloom, G. S. (2014). Amyloid-β and tau: The trigger and bullet in Alzheimer disease pathogenesis. *JAMA Neurology, 71*(4), 505–508. https://doi.org/10.1001/jamaneurol.2013.5847

Desai, B., Kushwaha, U., Jha, S., & NMIMS, M. (2020). Image filtering—Techniques, algorithms, and applications. *Applied GIS, 7*(2), 970–975.

Ebrahimighahnavieh, M. A., Luo, S., & Chiong, R. (2020). Deep learning to detect Alzheimer's disease from neuroimaging: A systematic literature review. *Computer Methods and Programs in Biomedicine, 187*, 105242. https://doi.org/10.1016/j.cmpb.2019.105242

Fang, C., Li, C., Cabrerizo, M., Barreto, A., Andrian, J., Rishe, N., Loewenstein, D., Duara, R., & Adjouadi, M. (2018). Gaussian discriminant analysis for optimal delineation of mild cognitive impairment in Alzheimer's disease. *International Journal of Neural Systems, 28*(4), 1850017. https://doi.org/10.1142/S0129065718500172

Feng, W., Halm-Lutterodt, N. V., Tang, H., Mecum, A., Mesregah, M. K., Ma, Y., Li, H., Zhang, F., Wu, Z., & Yao, E. (2020). Automated MRI-based deep learning model for detection of Alzheimer's disease process. *International Journal of Neural Systems, 30*(5), 2050032. https://doi.org/10.1142/S0129065720500323

Gunturk, B., & Li, X. (2018). *Image restoration*. CRC Press.

Jain, R., Jain, N., Aggarwal, A., & Hemanth, D. J. (2019). Convolutional neural network based Alzheimer's disease classification from magnetic resonance brain images. *Cognitive Systems Research, 57*, 147–159. https://doi.org/10.1016/j.cogsys.2018.12.015

Jensen, J. R., & Lulla, K. (1987). *Introductory digital image processing: A remote sensing perspective*. Prentice Hall.

Kaur, S., Gupta, S., Singh, S., & Gupta, I. (2022). Detection of Alzheimer's disease using deep convolutional neural network. *International Journal of Image and Graphics, 22*(1), 2140012. https://doi.org/10.1142/S0219467821400127

Koepsell, T. D., & Monsell, S. E. (2012). Reversion from mild cognitive impairment to normal or near-normal cognition: Risk factors and prognosis. *Neurology, 79*(15), 1591–1598. https://doi.org/10.1212/WNL.0b013e31826e25b4

Li, Z., Liu, F., Yang, W., Peng, S., & Zhou, J. (2021). A survey of convolutional neural networks: Analysis, applications, and prospects. *IEEE Transactions on Neural Networks and Learning Systems, 33*(12), 6999–7019. https://doi.org/10.1109/TNNLS.2021.3084827

Menikdiwela, M., Nguyen, C., & Shaw, M. (2018). Deep learning on brain cortical thickness data for disease classification. In *2018 Digital Image Computing: Techniques and Applications (DICTA)* (pp. 1–5). IEEE. https://doi.org/10.1109/DICTA.2018.8615763

Michelucci, U. (2018). *Applied deep learning: A case-based approach to understanding deep neural networks*. Apress. https://doi.org/10.1007/978-3-319-73004-2

Muniyappan, S., Allirani, A., & Saraswathi, S. (2013). A novel approach for image enhancement by using contrast limited adaptive histogram equalization method. In *2013 Fourth International Conference on Computing, Communications and Networking Technologies (ICCCNT)* (pp. 1–6). IEEE. https://doi.org/10.1109/ICCCNT.2013.6726614

Nawaz, A., Anwar, S. M., Liaqat, R., Iqbal, J., Bagci, U., & Majid, M. (2020). Deep convolutional neural network based classification of Alzheimer's disease using MRI data. In *2020 IEEE 23rd International Multitopic Conference (INMIC)* (pp. 1–6). IEEE. https://doi.org/10.1109/INMIC50486.2020.9318135

Ocasio, E., & Duong, T. Q. (2021). Deep learning prediction of mild cognitive impairment conversion to Alzheimer's disease at 3 years after diagnosis using longitudinal and whole-brain 3D MRI. *PeerJ Computer Science, 7*, e560. https://doi.org/10.7717/peerj-cs.560

Ongsulee, P. (2017). Artificial intelligence, machine learning and deep learning. In *2017 15th International Conference on ICT and Knowledge Engineering (ICT&KE)* (pp. 1–6). IEEE. https://doi.org/10.1109/ICTKE.2017.8259629

Owotogbe, J., Ibiyemi, T., & Adu, B. (2019). A comprehensive review on various types of noise in image processing. *International Journal of Scientific & Engineering Research, 10*(7), 388–393.

Padzil, F. M., & Crebbin, D. G. (2016). Linear and nonlinear filter for image processing using MATLAB's image processing toolbox. *Murdoch University*.

Salem, N., Malik, H., & Shams, A. (2019). Medical image enhancement based on histogram algorithms. *Procedia Computer Science, 163*, 300–311. https://doi.org/10.1016/j.procs.2019.12.103

Sarvamangala, D., & Kulkarni, R. V. (2022). Convolutional neural networks in medical image understanding: A survey. *Evolutionary Intelligence, 15*(1), 1–22. https://doi.org/10.1007/s12065-020-00540-3

Schwenk, K., & Huber, F. (2015). Connected component labeling algorithm for very complex and high-resolution images on an FPGA platform. In *High-Performance Computing in Remote Sensing V* (pp. 9–22). SPIE. https://doi.org/10.1117/12.2189062

Yang, C., Sun, X., Tao, W., Li, X., Zhang, J., Jia, J., Chen, K., & Zhang, Z. (2017). Multistage grading of amnestic mild cognitive impairment: The associated brain gray matter volume and cognitive behavior characterization. *Frontiers in Aging Neuroscience, 8*, 332. https://doi.org/10.3389/fnagi.2016.00332

Yousefi, J. (2011). Image binarization using Otsu thresholding algorithm. *University of Guelph*, 10.

Zhang, Y., Liu, S., & Yu, X. (2020). Longitudinal structural MRI analysis and classification in Alzheimer's disease and mild cognitive impairment. *International Journal of Imaging Systems and Technology, 30*(2), 421–433. https://doi.org/10.1002/ima.22402